PED-Vol. 18

# Sensors and Controls for Manufacturing

edited by

E. KANNATEY-ASIBU, JR.
A. G. ULSOY
R. KOMANDURI

# Sensors and Controls for Manufacturing

*presented at*

THE WINTER ANNUAL MEETING OF
THE AMERICAN SOCIETY OF MECHANICAL ENGINEERS
MIAMI BEACH, FLORIDA
NOVEMBER 17-22, 1985

*sponsored by*

THE PRODUCTION ENGINEERING DIVISION, ASME

*edited by*

E. KANNATEY-ASIBU, JR.
UNIVERSITY OF MICHIGAN

A. G. ULSOY
UNIVERSITY OF MICHIGAN

R. KOMANDURI
GENERAL ELECTRIC COMPANY

THE AMERICAN SOCIETY OF MECHANICAL ENGINEERS
United Engineering Center 345 East 47th Street New York, N.Y. 10017

Library of Congress Catalog Card Number 85-73232

# PREFACE

The ever increasing competition, higher costs and decreasing productivity are forcing the US industry to seriously re-evaluate their current manufacturing practices. This is leading to more and more automation as witnessed in recent years. The need to improve quality and decrease scrap rate while increasing the production rate is forcing industry to consider untended machining as a viable alternative. However, this leaves the operator, who also serves the crucial function of multi sensing and control of the manufacturing process adaptively, out of the manufacturing loop in many cases. Unfortunately, there are many variables that effect the manufacturing process. The operator attempts to sense the effect of these variables to the best of his ability and adjusts the conditions of the operation accordingly. Often-times, however, the operator is not in a position to sense the operation for a variety of reasons and/or incapable of responding fast enough to alter the conditions of operation. Consequently the operating conditions are generally chosen conservatively. The former leads to higher scrap rate and higher costs due to the need for rework. The latter leads to reduced productivity. Appropriate sensors and associated controls are, therefore, the key to the successful implementation of untended machining.

Several sensors have been evaluated with varying success over the past 30 years for their suitability in monitoring the cutting process. These include, among others, sensors based on force, torque, power, vibration, deflection, acoustic emission, vision, and radioactivity. However, the implementation of any of the above sensors was slow, if any, until recently due to marginal need and lack of acceptance on the manufacturing shop floor. Inadequate-reliability and lack of fast response control were the main reasons for the lack of acceptance of these systems for use on the manufacturing shop floor. Today, the need is felt more than ever and this will continue to grow if we were to be successful in implementing untended manufacturing efficiently. The availability of inexpensive but high power computers is enabling us to develop and implement fast but powerful sensor signature analysis systems and control strategies necessary for proper use of sensors. The quality and reliability of sensors are also improving continuously. There is hope that in the near future some reliable sensing and control systems will be available to meet the needs of untended manufacturing.

Of the various sensors evaluated thus far in machining, force, power, torque, acoustic emission and vibration sensors are showing some promise for application on the shop floor. These sensor systems have sophisticated software on analysing the data and for monitoring the process. The emphasis in research is now on the development of signal conditioning and monitoring and control strategies than on hardware. Most research institutions, involved in manufacturing be it industry or university, are working on sensor research.

The first objective of this symposium is to present the state-of-the-art research on this subject.

The second objective is to bring together researchers working on different sensor approaches for a dialogue on the pros and cons of different sensing and control systems for different applications.

The third objective of this symposium is to bring to the attention of the users the growing need to develop and implement sensing and control systems on the manufacturing shop floor so as to improve productivity and the quality of the parts. It may be pointed out that in some applications it is the lack of systems process monitoring that is preventing total automation, including non machining operstions.

The fourth and final objective of this symposium is to bring to the attention of users the outstanding capabilities and facilities available at universities to conduct sensor research which can lead to sensing and control systems that can be implemented on the shop floor. With the high cost of developing a product, US industry should team up with universities and other research institutions to make the best use of available resources.

These proceedings are a direct result of the original contributions of the authors and it is with pleasure that we acknowledge their valuable contributions. We also thank reviewers of the papers for their unselfish but valuable contributions. In conclusion, we sincerely hope that industry and university in general, and members of the Production Engineering Division of ASME in particular, can benefit from this work and the stimulating discussions at the symposium.

E. Kannatey-Asibu, Jr.,

A. Galip Ulsoy
Mechanical Engineering Department
University of Michigan
Ann Arbor, Michigan

Ranga Komanduri, Program Chairman PED
General Electric Company
Corporate Research and Development
Schenectady, New York

## CONTENTS

# VIBRATION MODES AND FREQUENCIES OF TWIST DRILLS USING USING LASER HOLOGRAPHIC INTERFEROMETRY

**J. C. MacBain,** Senior Researcher and **K. G. Harding,** Researcher
Industrial Technology Institute
Ann Arbor, Michigan

**O. Tekinalp,** Graduate Student
Department of Mechanical Engineering and Applied Mechanics
University of Michigan
Ann Arbor, Michigan

## ABSTRACT

Drilling is one of the most important and common machining operations carried out in the manufacturing of durable goods. It is important to understand the structural dynamic response of the drilling operation both in terms of drill-hole accuracy, as well as, drill wear and breakage. In this vein, knowledge of the drill's natural vibration modes and frequencies is essential, both in understanding the phenomena governing the drilling process, and in generating appropriate analytical models of the drill's structural dynamic behavior. Toward this end, this paper presents the results of an experimental study using laser holographic interferometry to record the natural mode shapes and frequencies of two stationary drills measured under simulated axial loads and with varying depth of drill hole. The experimental results are discussed in light of related analytical studies and compared to classical beam theory.

## INTRODUCTION

Modern industrial trends are leading more and more toward untended manufacturing processes. In the case of untended machining, drilling is one of the more important and most common machining operations. It is estimated, for example, based on figures from the Metal Cutting Tool Institute, that in 1984 companies in the United States purchased close to $375 million dollars worth of drills from domestic and foreign suppliers.

In order to carry out untended drilling operations successfully, it is important to understand the structural dynamic characteristics of the drilling process. This has a direct bearing on drill wear and breakage and on drill-hole accuracy. A vibrating drill can cause the drill hole to "wander" from its true center(1). Conversely, a worn drill or one subject to impending failure may give off a vibration signal indicating its deteriorating condition. This latter phenomenon has been investigated both as a "one-per-rev" wear signal(2) and in terms of a higher order frequency output(3). While neither study modeled the drill's mechanical response, knowledge of the drill's structural dynamic characteristics would have been helpful in understanding the governing phenomena.

Of paramount importance in characterizing the drill's structural response, is its resonant modes and frequencies of vibration. This problem has been addressed using a lumped parameter drill model under rotating conditions by Ulsoy and Tekinalp(4). The authors experimentally validated the lumped mass model for the fundamental frequency of a long, slender drill under rotating conditions. The problem of determining the drill's mode shapes and frequencies has also been addressed analytically by Magrab and Gilsinn(5) who modeled the drill as a twisted Euler beam under axial load that is clamped at both ends.

The purpose of the present paper is to shed some additional light on the actual nature of the modes and frequencies of a drill fixed in a typical drill holder acted upon by a representative axial load. For example, what are the actual boundary conditions at the drill-workpiece interface? What role, if any, does the drill holder play in the vibratory motion? Are the drill's lower mode shapes patterned after simple beam response or are they more complex?

Reported herein are the results of experimental tests carried out to determine a drill's resonant modes and frequencies of vibration using laser holographic interferometry. While the tests were carried out under static (nonrotating) conditions, the primary conditions present under actual drilling operations were simulated. These included, clamping conditions, depth-of-hole, and axial force, i.e., everything but rotation and torque due

to cutting force. The vibration modes and frequencies of two drills were studied, one with a 1/4-inch diameter and one with a 3/8-inch diameter. The drills were tested while being held by a typical tool holder and being subjected to a nominal axial loading, loading which could be expected under actual drilling conditions. The tests were run for various depths of penetration ranging from surface point (zero depth) to 1-inch depth. For purposes of comparison, a 3/8-inch diameter drill blank was also tested. The procedure for how this was accomplished and the graphical data that resulted will be described in the following sections.

## EXPERIMENTAL TEST SET-UP

As mentioned above, two twist drills of different diameters were used in the study. Both were standard HSS drills, one was 5.125 inches (130 mm) in length with a 3/8-inch (9.52 mm) diameter and the other was 4.125 inches (105 mm) in length with a 1/4-inch (6.35 mm) diameter. A drill blank, also tested, had the same properties as the 3/8-inch diameter drill. The drill tool holder was a Bridgeport Quick Change Collet (No. 30). The tool holder and drills are shown in Fig. 1.

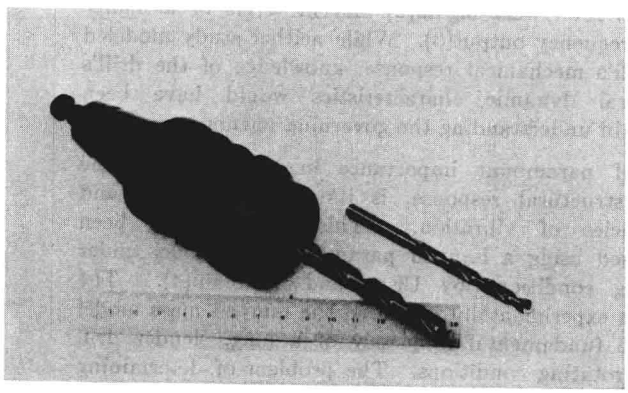

While vibration tests were performed in a nonrotating environment on a stable optics table, drilling tests were first run on a Bridgeport Series milling machining in order to determine the nominal axial load during typical drill operations. While the axial force is not significantly dependent on the rotational speed, it does depend on the feed rate(6,7). Consequently, the axial force was measured for the 1/4- and 3/8-inch diameter drills while drilling into a 1018 cold-rolled steel block. Different feed rates were used, the values being percentages of the recommended feed rates of .008 in/rev (.203 mm/rev) and .0092 in/rev (.234 mm/rev) for the 1/4- and 3/8-inch drills, respectively. The axial force was measured using a Kistler four-component dynamometer (Type 9273) placed under the steel block connected to a charge amplifier and strip chart recorder. The results of the tests are shown in Table 1. Based on these results, the axial force values of 1.05 kN and

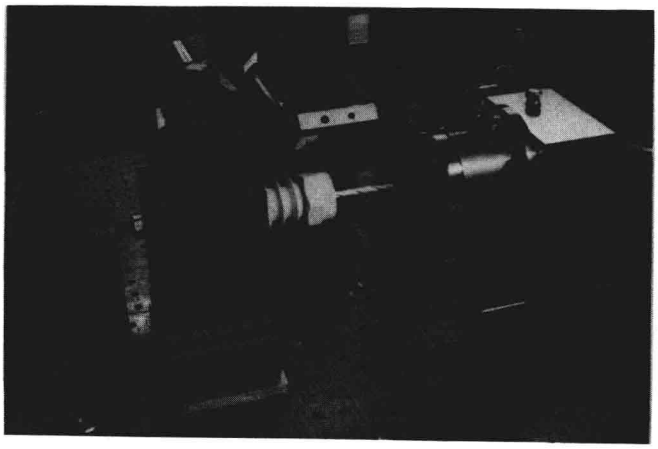

Fig. 2 Fixturing blocks and drill used for vibration tests

1.73 kN were used in the static vibration tests as the simulated axial loading for the 1/4- and 3/8-inch drills, respectively. For all of the tests, the drills were inserted 1 inch (25.4 mm) into the drill holder.

With the above information in hand, the drills and drill holder were placed in the fixture set-up shown in Fig. 2 in order to carry out the vibration tests.

A large steel block, denoted as "drill" block (B2 in Fig. 3), was bored out to accommodate the tapered shape of the Bridgeport drill holder. Using a threaded arrangement fixed to the back end of the drill holder, the drill holder could be drawn tightly into the drill block by turning a nut on the back of the steel block. In this way, the grasp of the Bridgeport milling machine on the drill holder could be simulated. In order to insure repeatability, the nut was always tightened to a torque of 38 ft-lbs (51 Nm) during the tests. The drill block was loosely bolted to the test table through slotted flanges at its base.

A second block, denoted as the "force" block (B1 in Fig. 3), containing a 3/8-inch diameter threaded rod lying on the same axis as the drill and drill holder, was placed directly to the left of the drill block so that the rod butted up against the back of the drill holder. By turning the 3/8-inch rod in the force block, the drill block could be made to move along the table.

To the right of the drill and drill block was a third block that we will denote as the "base" block (B3 in Fig. 3). It was rigidly bolted to the table. Fixed on the base block's side, colinear with the drill axis was the Kistler dynamometer. Attached to the dynamometer was a small steel test block having a hole in its center whose diameter matches that of the 1/4- or 3/8-inch drill. We will denote this last block as the "hole" block (BH in Fig. 3). The depth of hole varied from zero (center drill only) to 1/4-, 1/2-, and 1-inch depths. Hence, to cover both drill diameters for this series of hole depths, seven different blocks were needed.

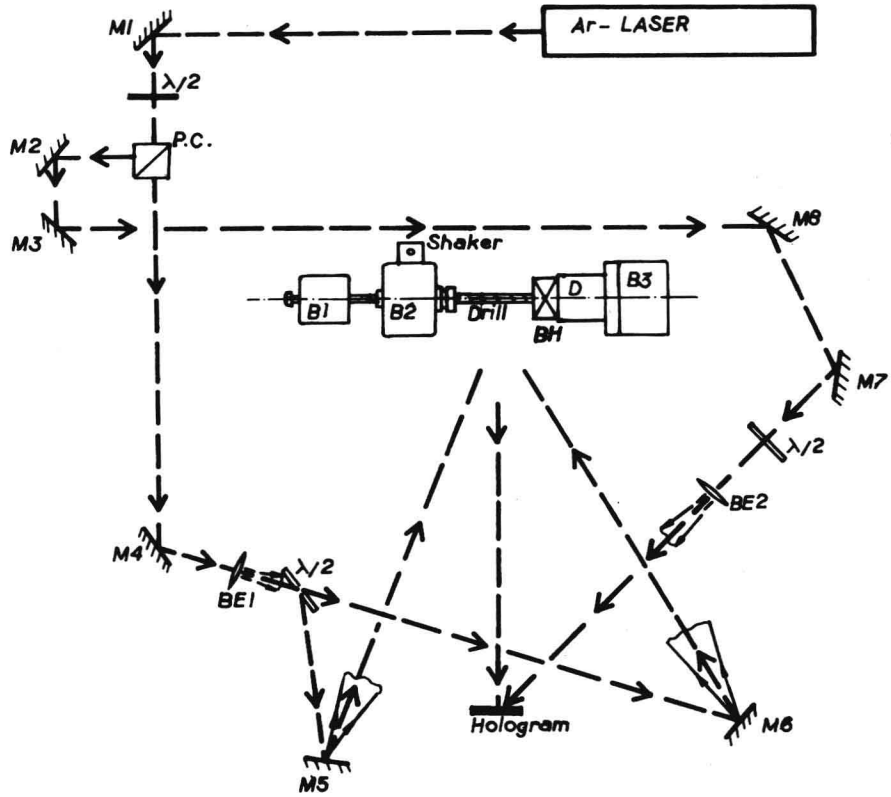


Fig. 3 Experimental set-up for carrying out holographic vibration tests: M1 through M8 - mirrors, BE1, BE2 - beam expanders, λ/2 - half-wave plate, P.C.-beam splitter, B1 - force block, B2 - drill block, BH - hole block, D - dynamometer, B3 - base block

The holes in the "hole" block were drilled using the same drills used in the vibration tests. The actual diameter for the 3/8-inch drill was measured to be .3743 inches (9.507 mm) and for the 1/4-inch drill to be .2495 inches (6.337 mm). The inside diameter of the drilled holes was 3.5-4.0 thousandths (.088-.101 mm) larger than the 3/8-inch diameter drill and 1-2 thousandths (.025-.051 mm) larger than the 1/4-inch diameter drill. This type of clearance is typical of that resulting from standard drilling processes and is due to asymmetries in the drill.

With all blocks lined up and in place so that the drill just contacted the bottom of the hole in the test block and so that the 3/8-inch diameter rod in the force block just contacted the back of the drill holder in the drill block, the 3/8-inch diameter rod could be turned causing an axial load to be imposed on the drill. This load was measured using the dynamometer and made to match the nominal axial loads found for the 1/4- and 3/8-inch drill during the drilling tests on the Bridgeport mill. The drill was now ready to be tested for its vibration modes and frequencies using holographic interferometry.

Holographic interferometry is an ideal method for experimentally determining the natural modes and frequencies of vibrating objects(8,9). It is particularly suited for analyzing objects that are relatively small and have complex geometries. This is the case of the twist drill. Point-by-point vibration analysis methods are very difficult to apply in ascertaining modes shapes of structures such as drills. The noncontacting technique of holographic interferometry is ideally suited for this purpose, yielding full-field recordings of the drill's mode shapes. The reader is referred to the references 8 and 9 for details.

A schematic of the experimental set-up is shown in Fig. 3. This is a typical off-axis holographic arrangement, with the small exception that two object beams were used to illuminate the object (drill, drill holder, and blocks) instead of one as is typically the case. This was done because either the drill block or the hole

Table 1 Axial force, $F_z$ vs. nominal feed rate, $f_n$

Material - 1018 cold-rolled steel, hardness = 85 $R_b$

| %$f_n$ | $F_z$ (kN) Drill dia. = 1/4 in. $f_n$ = .008 in/rev | Drill dia. = 3/8 in. $f_n$ = .0092 in/rev |
|---|---|---|
| 25 | .35 | .47 |
| 50 | .70 | .85 |
| 75 | .87 | 1.33 |
| 100 | 1.05 | 1.73 |
| 125 | 1.27 | 2.10 |

block would cause a shadow if a single object beam were used. The laser used for the tests was a 2-watt Argon-ion (Coherent Innova 90-3). One item that is somewhat different from the typical holographic set-up is that a mirror was placed at an angle of 45° over the drill (45° rotated parallel to the drill's axis). This was done so as to observe any motion of the drill in a direction vertical to the table. This would be in addition to out-of-plane motion perpendicular to the plane of the hologram that is normally observed using the technique.

The drill frequencies and modes were excited using a piezoelectric exciter (Jodon EV-100) attached to the side of the drill block opposite the hologram. For each of the configurations mentioned above (drill diameter, depth of hole, etc.), four to five modes and frequencies of vibration were determined and recorded. These are discussed in the following section.

## EXPERIMENTAL RESULTS

The natural frequencies for the drills at various hole depths are given in Tables 2 and 3 for the 3/8-inch and 1/4-inch diameter drills respectively. The mode shapes are denoted in the tables as "B" for bending and "T" for torsion. Thus, "2B" would be the second bending mode shape of the drill. One of the interesting results of the tests, was that there were modes of vibration where the drill and the drill holder responded together in a system mode. These were similar to the drill-alone modes, but occurred at frequencies different from the drill-alone modes. These are denoted by the bending or torsion nomenclature described above, followed by "holder" in parenthesis. Hence, at some frequencies, the drill holder acted as the classical "rigid support" and at others, it participated in the motion. A good example of this is shown in Fig. 6 below for the case of the first torsional mode.

It can also be seen from Tables 2 and 3 that not all of the modes were excited. Because of the relatively large stiffness and mass of the system, some of the modes could not be excited to an amplitude sufficient for recording. For the most part, however, the first and second bending modes and the first torsion mode were excited in each configuration. This is as it should be, since these lower modes respond more easily (they require less energy to excite) than the higher modes. As one would expect, the frequencies increase with increasing depth of drill hole. This is especially evident in the case of the first bending frequency. There was some deviation from this trend in some of the higher modes due to the variability of the boundary conditions. Note, for example, the results of the 3/8-inch diameter drill at 1/4-inch hole depth in Table 2. All frequencies for this case ran consistently higher due to some anomaly in the clamping conditions.

The second bending (2B) frequency shown in Table 3 for the 1/4-inch drill shows a rather interesting jump at the 1-inch hole depth to approximately twice its value of that at the 0-, .25-, and .5-inch depths. This mode was checked holographically and it was confirmed the natural frequency at 18,670 Hz was indeed the 2B mode shape of the drill. A possible reason for this jump in frequency is that for the shorter hole depths, the effective length of the drill is its total length from drill holder to drill tip, with only a slight effect due to the hole depth. (Recall that there is a $\pm$1-2 thousandths clearance between the drill and the hole.) At the 1-inch hole depth, however, one of the antimodes of the second bending mode is near the hole opening. If the displacement of the antimode is large enough, the drill will collide with the side of the hole at this point and the mode will jump to a lower energy level, one where the nodal line is at the collision point. Hence the effective length of the drill would change from 3.125 inches to 2.125 inches. The increase in frequency would be proportional to the ratio of the effective lengths squared, a factor of 2.16. Multiplying the 2B frequency of 9050 Hz (0-inch depth) by this factor yields a value of 19,548 Hz, a value quite close to the experimental test value of 18,670 Hz. This same explanation holds for the *drop* in frequency (2700 Hz) for the 1B mode of the 1/4-inch drill at the 1-inch hole depth when compared to the 1B frequencies at the .25- and .5-inch hole depths. For this mode the drill apparently had a shorter effective length for the .25- and .50-inch hole depths causing their 1B frequencies to be higher.

Shown in Figs. 4 and 5 are photos of representative mode shapes taken from time-average holograms made during the tests. Figure 4 shows holographic interferograms of the first five mode shapes found for the 3/8-inch diameter drill at zero depth, i.e., just the tip of the drill is touching the hole block. Figure 5 gives interferograms of the mode shapes for the same drill with a 1/4-inch hole depth. In both cases the axial force was 1.73 kN. Similar mode shapes were obtained for the 1/4-inch drill but are not shown here. A careful look at the figures will reveal that there are two images of the drill. The second image, at the top of each photo, is from the mirror placed over the drill at 45° to record motion in a direction vertical to the test table. The relative absence of fringes in this image with respect to the lower image indicates that most of the drill motion took place in the plane of the table perpendicular to the

Table 2 Natural frequencies for 3/8-in. dia. drill vs. hole depth, d

Axial load, $F_z$ = 1.73 kN, Free length, L = 4.125 - d, (in.)

| Mode | Hole Depth, d (in.) 0 | .25 | .50 | 1.00 |
|---|---|---|---|---|
| 1B | 2253 | 3082 | 3100 | 3705 |
| 1B (holder) | | 2470 | | |
| 2B | 6620 | 7440 | 6732 | |
| 2B (holder) | | | 3713 | |
| 3B | 12030 | 13545 | 12370 | 15260 |
| 3B (holder) | | | | 8083 |
| 4B | 16952 | 18463 | 17525 | 17650 |
| 4B (holder) | | | | |
| 1T | 8770 | 10320 | 11540 | 11510 |
| 1T (holder) | | | | |

Table 3 Natural frequencies for 1/4-in. dia. drill vs. hole depth, d

Axial load, $F_z$ = 1.05 kN, Free length, L = 3.125 - d, (in.)

| Mode | Hole Depth, d (in.) 0 | .25 | .50 | 1.00 |
|---|---|---|---|---|
| 1B | 2900 | 3226 | 3726 | 2700 |
| 1B (holder) | | 2470 | 2695 | |
| 2B | 9050 | 9180 | 9495 | 18670 |
| 2B (holder) | | | | |
| 3B | 15340 | 15260 | | |
| 3B (holder) | | 8130 | 8130 | |
| 4B | | | | |
| 4B (holder) | | | | |
| 1T | | | 15620 | 15000 |
| 1T (holder) | | 5425 | 5400 | 5430 |

observer (in and out of the plane of the figure). This was because the principal axis of the piezoelectric exciter was in this direction. The fringes on the surface of the drill and possibly on the drill holder indicate contours of constant out-of-plane displacement. The whitest fringes in the figures are nodal lines or points of zero displacement. For example, Fig. 4(d) shows the third bending mode for the 3/8-inch diameter drill. Nodal lines are located at the 1/3 and 2/3 span locations of the the drill. The drill holder on the left is also a nodal point as is the hole block on the right. Figure 4(c) shows the first torsion mode. Since the drill is twisting about its axis in this mode, the nodal line runs the length of the drill. Hence, torsional modes are readily discernible from bending modes using this procedure.

Figure 5(a) shows a first bending holder mode, 1B (holder). Two interference fringes can be seen on the drill holder. The contrast between drill-alone modes and drill/drill holder modes is shown quite graphically for the case of torsional vibration in Fig. 6(a) and (b). These modes were excited for the 1/4-inch diameter drill at .5-inch hole depth. The drill holder is exhibiting a very obvious first torsioned vibration at 5,400 Hz with the drill just behaving as a rigid body (Fig. 6(a)). In contrast, at 15,620 Hz, the drill is responding to its first torsional frequency and the holder is fixed (Fig. 6(b)).

The fringe information from the interferograms can be used to plot the drill's out-of-plane displacement. This was done for the case of the 1B (holder), and 1B, and 2B mode shapes for the 3/8-inch diameter drill in the 1/4-inch depth hole (Fig. 5(a), (b), and (c)). The results are shown in Figs. 7 for the 1B (holder) and 1B mode shapes and in Fig. 8 for the 2B mode shape. The plots are based on the relation between the out-of-plane displacement, W, and the holographic fringe number given by:

$$W = \frac{\lambda \Omega_i}{2\pi(Cos\,\theta_1 + Cos\,\theta_2)} \qquad (1)$$

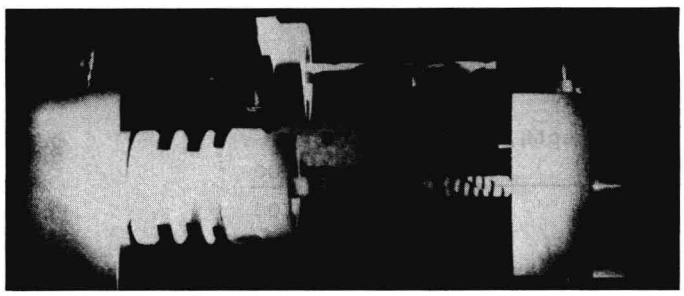

(a) 2253 Hz, 1B

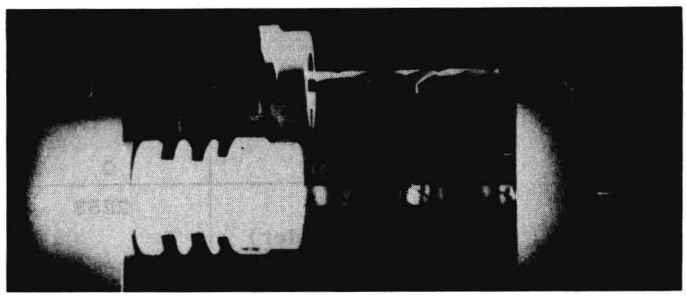

(b) 6620 Hz, 2B

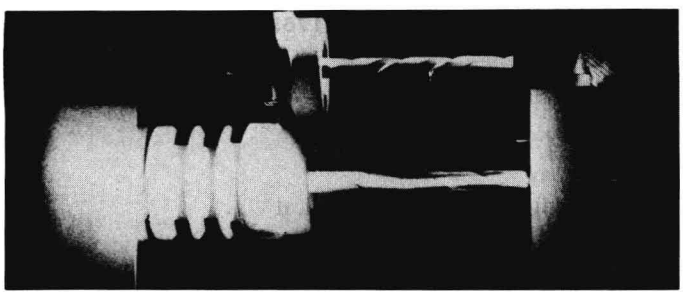

(c) 8770 Hz, 1T

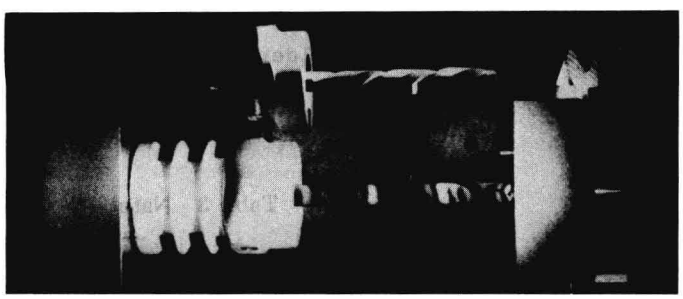

(d) 12030 Hz, 3B

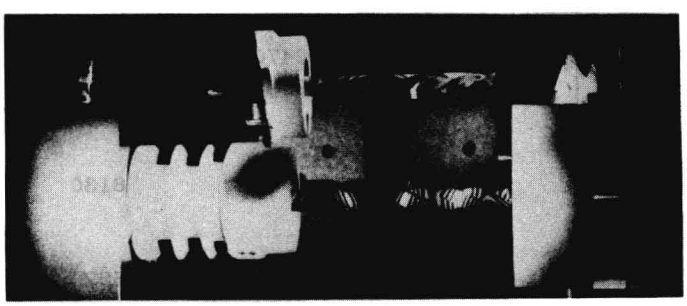

(e) 16952 Hz, 4B

Fig. 4 Vibration mode shapes and frequencies of 3/8-in. dia. drill at zero depth, $F_z = 1.73$ kN

where:

$\lambda$ - laser wavelength

$\Omega_i$ - i-th root of the zero order Bessel function, $J_o$, corresponding to the i-th fringe

$\theta_1$ - angle between the displacement vector of the drill and the line of observer/camera through hologram

$\theta_2$ - angle between the displacement vector of the drill and the laser "object" beam illuminating the drill.

For the current tests for both the front and top views of the drill: $\lambda = 20.2$ $\mu$in. (514 nm), $\theta_1 = O$, and $\theta_2 = 15°$. ($\theta_2 = 15°$ was based only on the object beam on the right since it was this beam that was the principal illumination for the drill.)

Looking at Fig. 7, one can see the relative difference between the drill's 1B (holder) mode and its 1B mode. For clarity, the abcissa for the plots in the figures is assumed to run from the origin at the drill holder-drill block interface to the point where the drill enters the hole block. Hence, except for the torsional mode shape, the nodal line that would normally appear on the far right at the drill tip is "buried" in the hold block. The displacement curves for the 1B and 2B drill-alone modes in the two figures are very similar to the classical 1B and 2B mode shapes for a clamped-clamped beam.

This brings us to the final, rather interesting, set of results of this study, the tests that were run on the drill blank and how they correlated with classical simple beam theory.

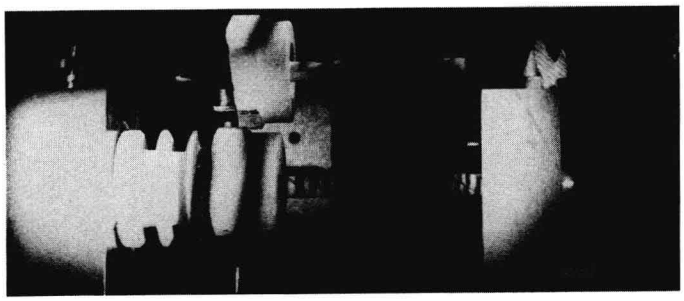

(a) 2470 Hz, 1B (holder)

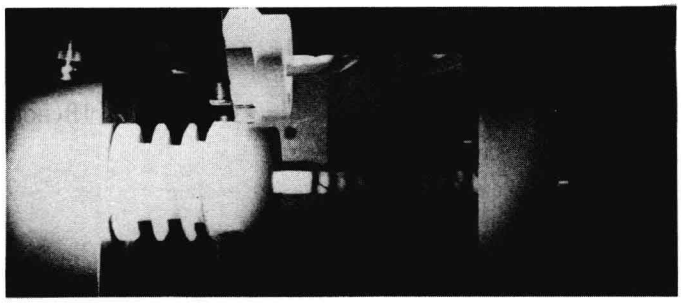

(b) 3082 Hz, 1B

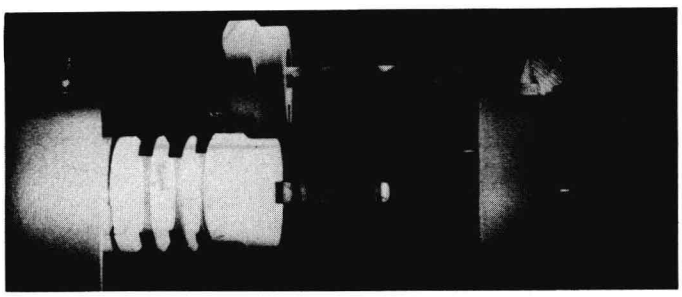

(c) 7440 Hz, 2B

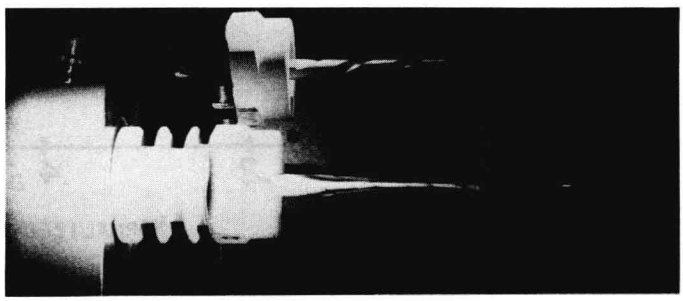

(d) 10320 Hz, 1T

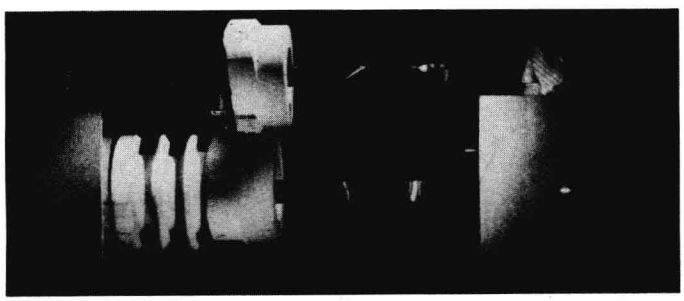

(e) 13545 Hz, 3B

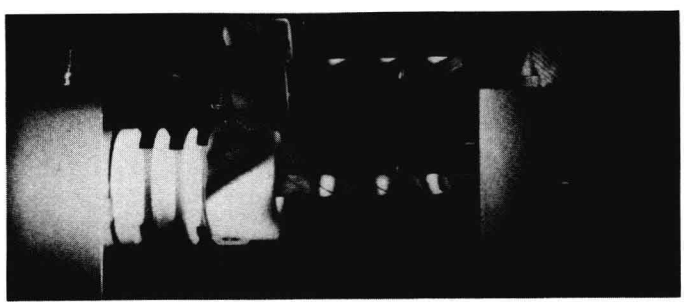

(f) 18463 Hz, 4B

Fig. 5 Vibration mode shapes and frequencies of 3/8-in. dia. drill at 1/4-in. hole depth, $F_z = 1.73$ kN

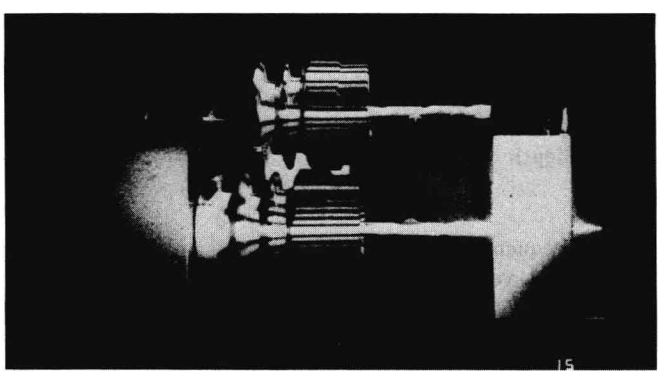

(a) 5400 Hz, 1T (holder)

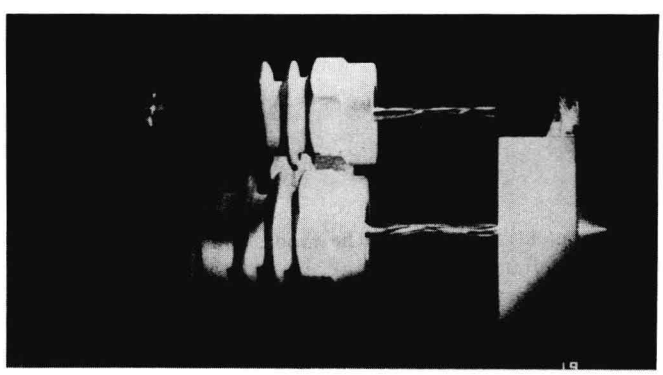

(b) 15620 Hz, 1T

Fig. 6 Drill-drill holder and drill-alone torsional mode shapes for 1/4-in. dia. drill at .5-in. hole depth, $F_z = 1.05$ kN

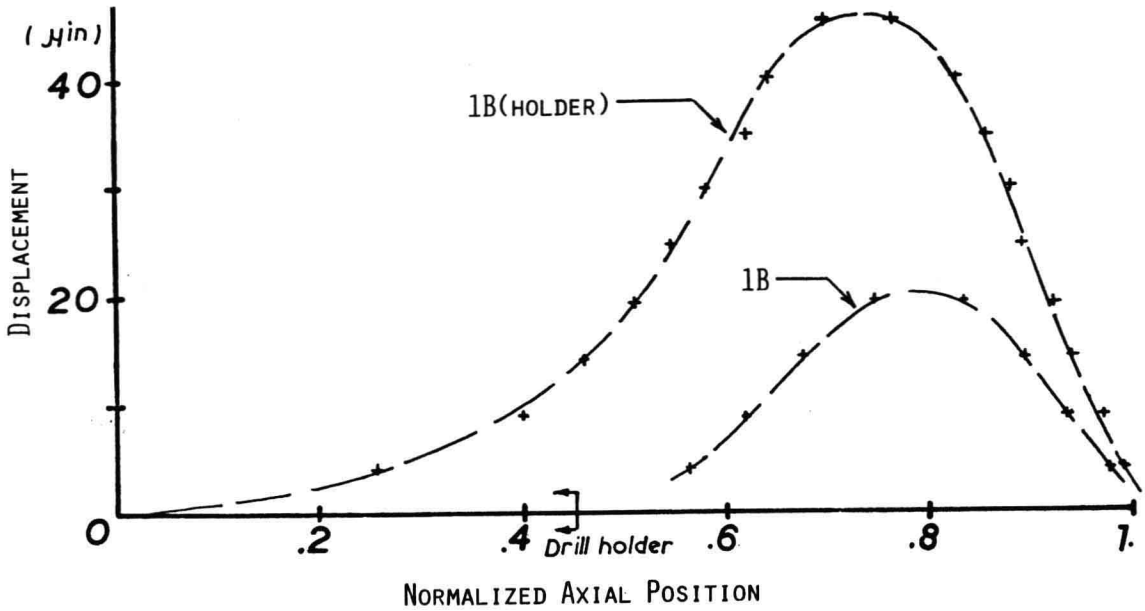


Fig. 7 Out-of-plane displacement for 1B (holder) and 1B mode shapes for 3/8-in. dia. drill in 1/4-in. hole depth

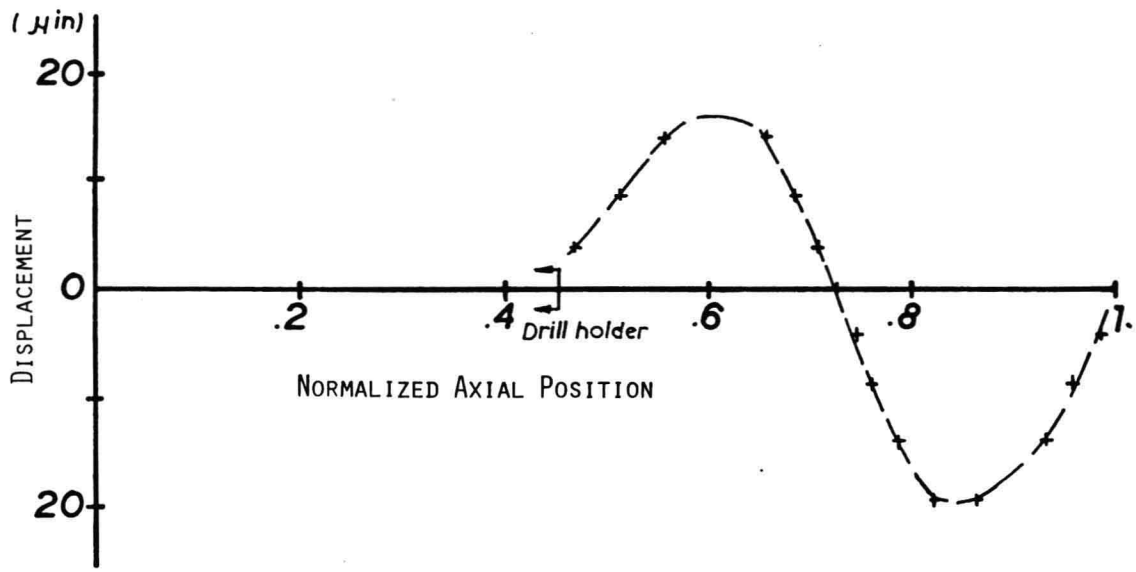


Fig. 8 Out-of-plane displacement for 2B mode shape for 3/8-in. dia. drill in 1/4-in. hole depth

As mentioned earlier, the modes and frequencies of a 3/8-inch diameter drill blank, i.e., a 3/8-inch diameter rod, were measured for the case of a 1/4-inch hole depth at a 1.73 kN axial load. The resulting frequencies are given in Table 4 for the first three bending modes and the first torsional mode. Also shown in the table, are values for the blank's natural frequencies based on simple beam theory under the assumption of clamped-clamped and clamped-hinged boundary conditions. It is interesting to note that while the two analytically derived sets of frequencies bracket the experimental set, the experimental values are closer to the clamped-clamped case than to the clamped-hinged case for the first bending and first torsion modes. In the case of the first bending mode, for example, the experimental value is 13% lower than its clamped-clamped counterpart while being 26% higher than the corresponding clamped-hinged value. For the second and third bending modes, however, the experimental frequencies are closer to the theoretical values for a clamped-hinged beam. Finally,

Table 4 Analytical vs. experimental frequencies for 3/8-in. dia. drill blank

Free length = 3.895 in. based on 1/4-in. hole depth

| Mode | Experimental* | Clamped-Clamped+ | Clamped-Hinged+ |
|---|---|---|---|
| 1B | 3720 | 4284 (4274)++ | 2948 |
| 2B | 10100 | 11797 | 9564 |
| 3B | 18075 | 23145 | 19942 |
| 1T | 14640 | 15252** | 7626** |

* Axial force, $F_z$ = 1.73 kN
** Based on free length of 4 in.
\+ No axial force
++ 1B frequency assuming a 1.73 kN axial force

the lower experimental frequencies are more likely due to clamping conditions than to axial load. This is because the values of the axial loads used in the study (based upon the drilling tests) are only a very small fraction of the drill buckling load. This is borne out by the 1B frequency computed for the clamped-clamped case under a 1.73 kN axial load. The frequency decreased by only 10 Hz below that of the unloaded case.

## DISCUSSION AND CONCLUSION

This paper has presented the results of experimental tests using holographic interferometry to determine the vibration characteristics of twist drills under simulated drilling conditions. The holographic results showed, quite explicitly, the nature of the drills' mode shapes.

Based on the mode shapes observed during the tests, it was found that, at least for the case of the lower modes, the drills responded in a manner quite similar to a simple beam model having either clamped-clamped or clamped-hinged boundary conditions. Both the bending modes and the torsional mode deformed in a manner that might be predicted using simple beam theory.

Based on the measured frequencies for the case of the drill blank, it was found the actual boundary conditions are closer to the classical clamped-clamped case for the first bend and first torsion modes but closer to the clamped-hinged case for the second and third bending modes. There is, however, some flexibility and/or clearance at the drill tip-hole interface. The effect of the clearance can cause nonlinear jumps to occur in the drill's natural frequencies that are dependent upon the drill's amplitude of vibration. There can also be some flexibility at the drill holder depending on the mass and stiffness characteristics of the holder. This last condition can lead to independent modes of vibration when the holder and drill act as one elastic structure.

Finally, as might be expected, the drills' natural frequencies show an increasing trend with increasing drill hole depth. The bending frequencies increase at a rate greater than the torsional frequencies.

The results reported herein are part of a larger study addressing the monitoring of drill wear and breakage. The present results will be used to identify the frequency spectra produced by both sharp and dull drills while drilling. The resulting spectra will be correlated with drill wear condition for possible use as a drill wear and breakage monitor. The results of this study shall be reported at a later date.

## ACKNOWLEDGMENT

The authors wish to express their appreciation for the excellent technical assistance and support provided by Dr. P. Balakrishnan and Mr. R. Tait of the Industrial Technology Institute. They also wish to thank Dr. A. Ber, visiting scholar to the Industrial Technology Institute, for his helpful technical advice.

## REFERENCES

1. Burnham, M.W., "The Mechanics of Drilling Small Holes," Manufacturing Engineering Transactions, 10th North American Manufacturing Research Conference Proceedings, Ontario, Canada, 1982.

2. Yee, K.W., and Blomquist, D.S., "An On-line Method of Determining Tool Wear by Time-Domain Analysis," SME Technical Paper MR82-901, 1982.

3. Braun, S., Lenz, E., and Wu, C.L., "Signature Analysis Applied to Drilling," Paper No. 81-DET-9, ASME Design Engineering Technical Conference, Hartford, Ct, September 20-23, 1981.

4. Ulsoy, A.G., and Tekinalp, O., "Dynamic Modelling of Transverse Drill Bit Vibrations," Annals of the CIRP, Vol. 33, No. 1, 1984.

5. Magrab, E.B., and Gilsinn, D.E., "Buckling Loads and Natural Frequencies of Drill Bits and Fluted Cutters," Paper No. 84-WA/Prod-12, ASME Winter Annual Meeting, New Orleans, La, December 9-13, 1984.

6. Shaw, M.C., and Oxford Jr., C.J., "On the Drilling of Metals," ASME Transactions, Vol. 79, Janurary, 1957.

7. Ber, A., Rotberg, J., and Gati, U., "Investigation of P.C.D. Drilling Parameters," Proceedings of the Superabrasive 85 Conference, Chicago, Illinois, April, 1985, pp. 48-91.

8. MacBain, J.C., Kielb, R.E., and Leissa, A.W., "Vibrations of Twisted Cantilevered Plates - Experimental Investigation," ASME Paper No. 84-GT-96, 29th International Gas Turbine Conference, Amsterdam, The Netherlands, June 4-7, 1984.

9. Vest, C.M., Holographic Interferometry, John Wiley & Sons, New York, New York, 1979.

# DYNAMIC MODELING AND ANALYSIS OF THE BORING MACHINING SYSTEM

**G. M. Zhang,** Graduate Research Assistant, and **S. G. Kapoor,** Associate Professor
Department of Mechanical and Industrial Engineering
University of Illinois at Urbana-Champaign
Urbana, Illinois

ABSTRACT

A system model formulated in the state variable space is proposed to describe the dynamic characteristics of the boring machining system. Particular attention is paid to the effect of the tangential vibration on the system performance. Modal analysis in the eigenvector space is employed to derive the analytical form of the system response. Experiments are carried out under spiral cutting conditions and the critical cutting stiffness predicted by the proposed model is compared with corresponding measured values, showing good agreements.

NOMENCLATURE

$A$ = system matrix of the system dynamic equations, 4 x 4

$B$ = input matrix of the system dynamic equations, 4 x 2

$C$ = output matrix for normal displacement, 1 x 4

$C_{1,2}$ = damping factor of the two principal modes

$C_s$ = lead angle of tool

$D$ = output matrix for tangential displacement, 1 x 4

$d$ = depth of cut, mm

$f$ = feed, mm/rev

$G(s)$ = Laplace form of open-loop transfer function

$G(j\omega)$ = complex form of open-loop transfer function

$g_1(s)$ = Laplace form of structural dynamics of mode 1

$g_2(s)$ = Laplace form of structural dynamics of mode 2

$K_{1,2}$ = static stiffness of the two principal modes

$K_c$ = cutting stiffness

$K_v$ = gain factor related to cutting velocity variation

$K_p$ = gain factor related to penetration rate

$K_t$ = gain factor related to tangential vibration

$M$ = equivalent mass of boring bar structure

$M(s)$ = Laplace form of closed-loop transfer function

$M(j\omega)$ = complex form of closed-loop transfer function

$N$ = spindle speed of workpiece, rpm

$P$ = transformation matrix, 4 x 4

$\underset{\sim}{Q}(t)$ = state vector in the eigenvector space, 4 x 1

$T$ = time duration of one revolution

$u_o$ = normal uncut chip thickness, $f^* \cos C_s$, mm

$u(t)$ = chip thickness or the magnitude of step input function, mm

$\underset{\sim}{u}(t)$ = matrix form of input function, 2 x 1

$W$ = width of cut, mm

$\underset{\sim}{X}(t)$ = state vector (displacements and velocities of two principal modes), 4 x 1

$y(t)$ = relative displacement between tool and workpiece normal to machined surface

$y_{res}(t)$ = uncut chip thickness of the residual chip load left in the previous revolution, mm

$z(t)$ = relative displacement between tool and workpiece tangential to machined surface

$z_o$ = tool dynamic equilibrium position in tangential direction

$\Delta z(t)$ = variation of tool position with respect to tangential dynamic equilibrium position

$|\Delta z(t)|$ = magnitude of $\Delta z(t)$

$\omega = 2\pi f$ = angular frequency, rad/sec

$\omega_{1,2}$ = imaginary parts of the eigenvalues, or damped natural frequencies

$\sigma_{1,2}$ = real parts of the eigenvalues

$\theta$ = directional angle of the dynamic cutting force component

$\alpha$ = directional angle of the first principal mode

$\Phi$ = state transition matrix in the eigenvector space

$\Phi_{1,2}$ = phase shifting angles in the eigenvector spaces

## INTRODUCTION

The boring machining operation is widely used in industry. It is usually an enlarging operation, sizing and finishing an existing hole that has been drilled, forged, punched or cored. In the boring operation, the boring bar has to extend into the hole, and the length-to-diameter ratio of the boring bar could be large. Because of this, the stiffness of the boring bar is usually low and the boring bar becomes the weakest part in the machining operation. Any dynamic cutting force variation during machining can easily excite the operating boring bar. The result of this is either an inaccurate machining or an unstable cutting process.

The boring machining system has been studied for decades by many researchers. Many mathematical models have been proposed to describe the dynamic characteristics of the boring machining system (1,2,3,4). In a theoretical analysis of the boring machining system, Tlusty and Polacek developed two principles of mode coupling and regenerative effect in two subsequent cuts to study the system stability (1,3). The effects of cutting dynamics in terms of the dynamic cutting force components related to the instantaneous chip thickness variation and the penetration rate were further investigated by Parker (4). Using the models developed earlier (1,3,4), schemes of actively controlling the boring tool motion on-line were attempted (5,6). Difficulties, however, were met in the hardware realization.

In most of the previous approaches, the boring bar structure is represented by a lumped mass-spring-damper system (see Fig. 1a), and the dynamic cutting force is mainly related to the motion of the lumped mass in the direction normal to the machined surface. However, the boring bar vibrates or deforms during machining in both the normal and the tangential directions with respect to the machined surface. The deformation energy state of the boring bar during machining, which may cause system instability, is thus related to the motion of the lumped mass in both the normal and the tangential directions. More recently, Brown and Hinds (7) have shown that the direction of the dynamic cutting force tends to be along the tangential direction when machining materials such as titanium alloys. Under these circumstances, there will be a wide range of cutting conditions over which the tangential vibration instability will be encountered. Therefore, the tangential vibration instability which has been observed by many authors (4,5) cannot be predicted by previously developed models.

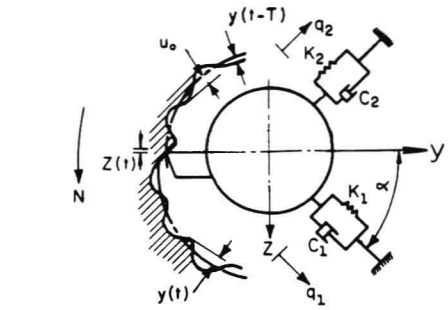


(a) Model of Two-Degree-of-Freedom

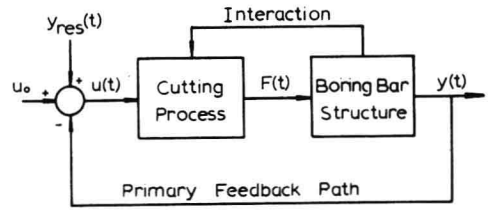


(b) Subsystems and Feedback Mechanism

Fig. 1 Boring Machining System

The purpose of this paper is to develop a new linear state variable system model for the boring machining system. The dynamic cutting force component accounting for the effect of the tangential vibration on the system performance is under consideration. The significance of the tangential vibration instability in the boring process is discussed in detail. By employing the modal analysis, an analytical form of the system response, namely, the tool motion, is derived for the prediction of the boring bar chatter during machining. Experiments under spiral boring conditions are conducted to experimentally obtain the limit width of cut and the results are compared with the corresponding predicted values from the new system model.

## DYNAMIC MODELING

A boring machininig system consists of a cutting process subsystem, a boring bar structure, and a feedback mechanism which forms the link between the cutting process subsystem and the boring bar structure as shown in Fig. 1b. The output and input pair of the boring machining system is conventionally defined as a pair of the displacement of the tool motion in the direction normal to the machined surface and the chip thickness to be cut, i.e. the uncut chip thickness.